Editors' Suggestion

When more is less: Higher magnetic fields and their limited impact on signal-to-noise ratio per unit of acquisition time in unlocalized and single-voxel magnetic resonance spectroscopy

Guodong Weng [1,2,3,*] and Johannes Slotboom [1,2,†]

[1] *Institute for Diagnostic and Interventional Neuroradiology, Inselspital, University Hospital and University of Bern, Bern, Switzerland*

[2] *Translational Imaging Center, sitem-insel, Bern, Switzerland*

[3] *Department of Radiology & Biomedical Imaging, Yale University, New Haven, Connecticut, USA*

(Received 11 April 2025; revised 7 August 2025; accepted 29 August 2025; published 21 November 2025)

Magnetic resonance spectroscopy (MRS) offers significant diagnostic potential but is inherently constrained by a low signal-to-noise ratio (SNR). While increasing the main magnetic field strength B_0 is theoretically linked to increased SNR, practically obtained gains in SNR from $B_0^{7/4}$ to B_0, depending on the domination of thermal noise at high B_0, are not always realized. Especially in clinical settings, the maximum reachable SNR is further constrained by the total available acquisition time (TA) and the regulatory limits on maximum tolerable specific absorption rate (SAR). This work attempts to derive mathematical expressions that enable systematic analysis of the theoretically achievable SNR gain. One important notion in this context is the SNR gain per unit of measurement time as a function of the main magnetic field B_0 strengths in the case of unlocalized X-nuclei and localized (1H and X-nuclei) single-voxel spectroscopy (SVS) pulse sequences. Our findings indicate that, under given fixed total amount of (patient acceptable) measurement time TA and maximum tolerable SAR limitation, together with conditions that ensure the adiabaticity of specific sequences, there exists an optimal magnetic field strength B_0 that maximizes SNR per unit of measurement time (SNR_t). Beyond this optimal B_0, further increases in field strength do not yield proportional improvements in SNR_t. Key factors are identified, including rf-pulse bandwidth scaling with B_0 and longitudinal relaxation time (T_1) dependencies, that impact the net gain as well. Our theoretical analysis emphasizes critical considerations for optimizing SNR per unit time in clinical MRS, even challenging the presumption that higher magnetic fields B_0 always yield improved SNR per unit of measurement time performance.

DOI: 10.1103/j138-v9gr

I. INTRODUCTION

From the early days of magnetic resonance imaging (MRI), it was understood that its signal-to-noise ratio (SNR) increases with the main magnetic field strength B_0, as the equilibrium magnetization M_0 scales linearly with B_0 under thermal equilibrium conditions. Edelstein *et al.* formalized this relationship, showing that, under sample-noise–dominated conditions, intrinsic SNR is proportional to B_0 [1]. Empirical studies confirmed approximately linear SNR gains from 0.5 T to 1.5 T, contributing to the widespread adoption of 1.5 T as the clinical standard in the 1990s. The motivation to move beyond 1.5 T was driven by the potential to trade higher SNR for improved spatial resolution or reduced acquisition time. A 2003 editorial observed that "one of the most obvious benefits [of higher field] is improved SNR," noting that while practical gains might be somewhat limited by hardware, further technological progress would help realize the full potential of ultrahigh field systems [2]. Higher fields were also promoted in magnetic resonance spectroscopy (MRS), where the benefits include not only increased SNR but also improved spectral resolution and larger chemical shift dispersion [3]. These expectations fueled the development and clinical introduction of 3 T systems, followed by research explorations at 4 T, 7 T, and beyond.

While basic theory indicated above suggested linear SNR scaling with magnetic field B_0, more advanced electromagnetic models predict superlinear behavior at ultrahigh field strengths, depending on coil geometry, tissue

*Contact author: guodong.weng@unibe.ch

†Contact author: johannes.slotboom@insel.ch

Published by the American Physical Society under the terms of the Creative Commons Attribution 4.0 International license. Further distribution of this work must maintain attribution to the author(s) and the published article's title, journal citation, and DOI.

properties, and wavelength effects. Simulations show that, in the human head, SNR may scale as $B_0^{2.1}$ centrally and $B_0^{1.2}$ near the surface. Experimental data supported this: Pohmann *et al*. observed ∼3.1× SNR gain from 3 to 7 T and ∼1.76× SNR from 7 T to 9.4 T, which both exceed linear expectations [4]. Similarly, Vaughan *et al*. found SNR at 7 T followed the trend from 1.5 to 4 T, with a ∼2.3× gain over 3 T [5], reinforcing the notion that ultrahigh fields can offer significantly enhanced sensitivity under optimal conditions.

At 7 T, the radiofrequency (rf) B_1^+ field inhomogeneity becomes pronounced due to the shorter rf wavelength in tissue, causing spatially varying flip angles. While parallel transmission and rf shimming help mitigate this, they add complexity [6]. Susceptibility effects also worsen with increased field strength, leading to image distortions and a faster transverse relaxation time T_2. Additionally, longitudinal relaxation time T_1 increases markedly (e.g., from ∼1.1 s at 3 T to ∼2.0 s at 7 T), which can reduce SNR if repetition times are not lengthened accordingly: Glover noted that a longer T_1 can lower SNR under fixed-time constraints, limiting the efficiency of ultrahigh-field imaging [7].

Another issue playing an important role is specific absorption rate (SAR) and regulatory constraints: at higher fields, like 7 T, SAR increases approximately with B_0^2, limiting the use of rf-intensive sequences. Regulatory thresholds (e.g., 3.2 W/kg head-average) often force a longer repetition time (TR), fewer slices, or lower flip angles to stay within safe limits. Ladd *et al*. noted that SAR offers "no upside" at high field—only constraints such as prolonged scan times and reduced protocol efficiency [6].

High-field 1H MRS at 7 T offers higher SNR and improved spectral resolution but adiabatic rf pulses, essential for robust excitation and refocusing, impose high SAR, especially when combined with magnetic field gradients. Slice-selective adiabatic refocusing pulses, as used in (semi)SADLOVE technique introduced by Slotboom in 1991 [8] and later renamed (semi)LASER [9], are particularly SAR-demanding. Amplitude-modulated broadband pulses (as in PRESS [10]) are not viable at 7 T due to bandwidth and SAR constraints [6]. As a result, clinical MRS at 7 T is often limited by the need to reduce flip angles or extend TR to remain within SAR safety margins.

An alternative is to eliminate magnetic field gradients during refocusing. The SLOW-method, introduced by Weng *et al*. (2022) [11], uses frequency-selective adiabatic full-passage pulses played out without gradients, which significantly reduces SAR to refocus "only" the chemical shift range. This contrasts with the earlier SADLOVE (LASER), where slice selection is achieved by applying adiabatic pulses in the presence of magnetic field gradients [8], which require much more rf bandwidth to keep the chemical shift displacement artifact within bounds. SLOW enables whole-brain spectral editing with high spatial and spectral quality while operating within SAR limits—an approach well-suited to ultrahigh field magnetic resonance spectroscopic imaging (MRSI).

Our experience with developing SLOW directly motivated us to explore more deeply how SNR behaves at ultrahigh field. We began to question whether SNR continues to increase indefinitely with B_0, or whether it may eventually plateau or even decline due to limitations imposed by SAR, relaxation times, and physiological constraints. This question served as the foundation for the theoretical and numerical analysis presented in this manuscript.

II. THEORY AND METHODS

A. Background

Magnetic resonance spectroscopy is inherently characterized by a low signal-to-noise ratio [12–14], even for protons, which possess the highest gyromagnetic ratio *and* natural abundance. Since the SNR of the MR signal increases with the main magnetic field strength B_0, MRS should ideally be performed at the highest possible magnetic field strength; marketing of the MR scanners with higher B_0 follows this simplistic assumption. The following relation between the magnitude of the equilibrium magnetization M_0 and the main magnetic field B_0 exists [15]:

$$M_0 = N\,\gamma^2\hbar^2\,I(I+1)B_0/3k_BT_s, \tag{1}$$

in which N is the number of spins, γ is the gyromagnetic ratio, $\hbar$ is the reduced Planck constant, I is the spin quantum number I ($I = ½$ for protons), k_B is the Boltzmann constant, and T_s is the temperature of the spin system. In the case when the equilibrium magnetization M_0 is excited by 90° by an rf pulse, and flipped into the transverse plane ($M_{xy} = M_0\sin(\pi/2)$), it induces a voltage in the receiver coil, proportional to the transverse magnetization M_{xy}, which is given by

$$S_{NMR} \propto d\boldsymbol{M}_{xy}/dt \propto \omega M_{xy}. \tag{2}$$

Since, in Eq. (2), $\omega = \gamma B_0$, it implies that the nuclear magnetic resonance (NMR) signal strength scales with B_0^2.

This theoretical relationship leads MR scanner manufacturers to promote midfield (MF) and ultrahigh field (UHF) scanners based on their ability to achieve higher SNR. However, in practice, the relationship appears to be more nuanced. Previous experimental work has demonstrated the close to ideal SNR gain (60–100%) for MRI and MRS with a long repetition time (TR) (5000 ms), from 4 to 7 T, for water [5] and metabolites [3]. In contrast, other studies measuring metabolite SNR using SVS/CSI MRS,

with shorter TR (1500–3000 ms), have shown less SNR gain (23–73%) from 1.5 to 3 T, provided that the same TR and TA are compared, as shown in previous reports [16–19]. In addition, a few studies report on a metabolite SNR gain of 20–60%, with TR of 3000–7000 ms, from 3 to 7 T [20–22]. These findings may give the impression that higher magnetic field strength *always* results in increased SNR, although practical measurements often reveal more complex dependencies. However, through theoretical analysis, this paper demonstrates that evaluating SNR *per unit acquisition time* (denoted by SNR_t) provides a more meaningful metric for clinical MRS applications than plain SNR. Given that the total patient scan time is typically limited to (at most) one hour, the available total acquisition time (TA) for spectroscopic exams in our institute and other sequences is limited to a maximum of 10–15 min. The SNR per unit of the acquisition time, which effectively normalizes the achievable SNR by the square root of TA, is therefore the most relevant parameter for optimizing the SNR of clinical MRS measurements, given a maximum total tolerable acquisition time.

Historically, there was an open question about whether higher field MR scanners (e.g., 1.5 and 3 T) were inherently better for clinical applications than their lower field counterparts. Low field systems offer advantages such as reduced cost, smaller footprint, lower power consumption, more flexible bore configurations, and improved safety profiles [23]. Although initially debated, the substantial SNR gain per unit time at higher fields, which enabled faster imaging, higher resolution, enhanced contrast sensitivity, and the development of advanced pulse sequences, ultimately resolved the controversy in favor of higher field systems [24]. A valid question that arises, however, is whether the SNR_t *always* increases with increasing magnetic field strength B_0?

Experimentally linear SNR per unit time gain with respect to B_0 have been reported in the past for fast MRSI with the correction of relaxation effects and a time-domain matched filter [25,26]. However, a theoretical analysis on the relationship between the SNR *per unit of acquisition time* with respect to B_0 has been lacking.

Therefore, this paper systematically analyzes the theoretical limitations and gains of *in vivo* MRS signals as a function of increasing magnetic field strength B_0, contrasting ultrahigh-, mid-, and low-level fields. More concretely, it examines to what extent the theoretical SNR_t improvement of the MR signal can be obtained in reality. Additionally, it investigates how factors like, e.g., total available acquisition time or specific absorption rate limitations [6,27] influence the practical obtainable SNR_t in a typical SVS sequence. Given the fact that the local and global SAR [6,28] increases with increasing B_0, the effect of B_0 is also included in the analysis. It is essential to emphasize that the intended rf-pulse flip angles are perfectly achieved.

B. Johnson–Nyquist noise (thermal noise)

Thermal noise in MRS/MRI arises mainly from two components: the thermal motion of charged particles within the measured sample (e.g., patient tissue) and the receiver coil. The induced noise power per hertz (Ψ^2) is given by [1,29–31]

$$\Psi^2 = 4k_B(R_sT_s + R_cT_c), \tag{3}$$

where k_B is the Boltzmann constant, R_s and R_c are the equivalent noise resistance of the sample (e.g., living tissue) and the receiver coil, respectively, and T_s and T_c are the thermodynamic temperatures of the sample and the receiver coil, respectively. It has been established that [1]

$$R_s \propto \omega^2 \propto B_0^2, \tag{4}$$

$$R_c \propto \sqrt{B_0}. \tag{5}$$

Therefore, we find the following:

$$\Psi^2 \propto (T_sB_0^2 + \alpha T_cB_0^{1/2}), \tag{6}$$

where α is the coil and preamplifier noise contribution coefficient, representing the additional noise sources beyond the sample. The relative noise contribution of the coil to the total noise is larger at low main magnetic field since it is proportional to $B_0^{1/2}$. For fields higher than 0.24 T (10 MHz for proton) [1,15], the noise contribution from the coil is negligible compared with that from the sample, allowing the second term to be ignored, so that

$$\Psi \propto B_0. \tag{7}$$

C. Pulse-sequence-dependent signal and noise levels

Different types of pulse sequences influence the observed signal intensities and noise levels. For unlocalized X-nuclei and localized (1H and X-nuclei) single-voxel spectroscopy (SVS) sequences such as PRESS [10] and (semi)SADLOVE/LASER [8,9], the factor σ_{seq} influencing the final observable SNR is given in Ref. [1], i.e.,

$$M_0\sqrt{NT_{sp}}F \propto n\sqrt{NT_{sp}}F = \rho\Delta V\sqrt{NT_{sp}}F = \sigma_{seq}, \tag{8}$$

in which ΔV is the volume of the spectroscopic voxel (assuming a homogeneous spin density ρ), n is the number of spins, N is number of excitation (sequence repetitions), T_{sp} is the total sampling time, and F is a pulse-sequence-dependent weighting function that depends on the pulse sequence parameters (TR), echo time (TE), and inversion time (TI), and also the longitudinal relaxation time T_1 and transverse relaxation time T_2. This weighting function F directly influences the MR-signal amplitudes of the metabolites and plays a central role in the computation of the SNR. Moreover, note that σ_{seq} is the SNR per square root of frequency units $\left(\text{i.e., } 1/\sqrt{Hz}\right)$.

D. *F*-factor and Ernst angle

It is important to note that this F-factor accounts for the *saturation* effects of the spin system under investigation. For one single unlocalized or SVS signal acquisition applied on the equilibrium state magnetization M_0, the value of $F = 1$. If the SNR of one single MRS measurement is insufficient, the pulse sequence must be repeated and the SNR must be improved by signal averaging. Let TR represent the sequence repetition time of the sequence and T_1 the longitudinal relaxation time of the spin system under investigation. When TR is less than approximately five times the value of T_1, the spin system does not fully relax to the ground state, resulting in an equilibrium longitudinal magnetization $M_z < M_0$ and, consequently, $F < 1$. In such cases, the optimal SNR cannot be achieved with a 90° flip angle. Instead, a smaller flip angle is required, known as the Ernst angle θ_E (named after Nobel Laureate Richard Ernst), which maximizes the SNR under these conditions.

For an SVS sequence without selective inversion (i.e., a nonsaturation inversion MRS experiment) and ignoring T_2 transverse relaxation effects, an excitation pulse with a flip angle θ equal to the Ernst angle θ_E results in a *maximum* F-factor given by

$$F = \frac{1 - e^{-\mathrm{TR}/T_1}}{1 - \cos\theta_E \cdot e^{-\mathrm{TR}/T_1}} \sin\theta_E, \tag{9}$$

$$\theta_E = \arccos(e^{-\mathrm{TR}/T_1}). \tag{10}$$

E. SNR

Combining Eqs. (7) and (8), the SNR of an SVS acquisition can be expressed as follows:

$$\mathrm{SNR} = \frac{S_{NMR}\sigma_{seq}}{\Psi} \propto B_0\sigma_{seq} = B_0\rho\ \Delta V\sqrt{NT_{sp}}F, \tag{11}$$

where S_{NMR} is the obtainable NMR signal from the perspective of physics and hardware and is related to the main magnetic field strength [1], i.e., the induced noise power per hertz (Ψ^2 is described in references [1,29,30], and σ_{seq} is a factor that is dependent on the MRS sequence parameters, which determine the observable signal intensities and noise levels of the hardware and subject.

It is important to note that, in this work, SNR is considered in the time domain rather than the frequency domain. This distinction is critical, as spectral linewidth broadening at higher field strengths can obscure SNR gains in the frequency domain [32,33]. In contrast, time-domain SNR remains a reliable and informative metric for evaluating theoretical performance limits. Our objective is to quantify the upper bound of SNR gain per unit acquisition time, for which time-domain SNR provides the most appropriate basis.

F. SNR per unit time of acquisition time (assuming a fixed TA)

From a clinical perspective, the total acquisition time for a sequence is of great importance. This is because the maximum total scan duration for a patient in an MR scanner should be (by all means) tolerable, i.e., approximately one hour, during which all the necessary sequences must be completed to address the clinical questions. For a sequence to be feasible in a clinical setting, its acquisition time (TA) should ideally remain below 10 min, in order to minimize patient discomfort, reduce motion artifacts, and maintain reasonable examination throughput—particularly when spectroscopy is performed alongside standard imaging protocols. This implies that TA for clinical sequences is essentially fixed. Consequently, it becomes crucial to evaluate the SNR per unit time of acquisition time SNR_t under the constraint of a fixed TA and assess the effective SNR gain or loss as a function of magnetic field strength B_0. The total acquisition time is expressed as (with N being the number of sequence repetitions):

$$TA = N\ \mathrm{TR}. \tag{12}$$

For an SVS sequence, the SNR per unit time while keeping TA fixed (denoted as $\mathrm{SNR}_t|_{TA}$) is given by

$$\mathrm{SNR}_t|_{TA} = \frac{\mathrm{SNR}}{TA} \propto \frac{B_0\sqrt{N}F}{TA} = \frac{B_0\sqrt{TA/\mathrm{TR}}F}{TA} \propto \frac{B_0F(B_0)}{\sqrt{\mathrm{TR}}}. \tag{13}$$

G. Specific absorption rate

The specific absorption rate measures the rate at which radiofrequency (rf) energy is absorbed by human tissue during an MRI or MRS(I) examination. It is a crucial safety parameter, i.e., the standard IEC 60601-2-33 [34], since excessive rf exposure can lead to tissue heating and potential physiological effects. To ensure patient safety, regulatory limits on SAR restrict the rf power that can be applied, which in turn affects the choice of pulse sequences and overall acquisition efficiency. The specific absorption rate quantifies the rf power absorbed per unit mass of human tissue, with the SI units of J kg^{-1} sec^{-1}. A simplified 2D model (illustrated in Fig. 1) describes SAR as follows [27,35]:

$$SAR = \frac{\sigma A^2\omega^2 \int_0^{T_p} B_1^+(t)^2 dt}{2m\ \mathrm{TR}} = \frac{E}{2m\ \mathrm{TR}}, \tag{14}$$

where σ is the electrical conductivity of tissue, A is the area of conductive loop, ω is the rf frequency (assumed constant), $B_1^+(t)$ is the rf amplitude, m is the tissue mass, T_p is the pulse duration, TR is the repetition time, and E is the rf-pulse energy. Note that Eq. (14) is valid under the assumption that, for a piecewise continuous rf pulse, changes in

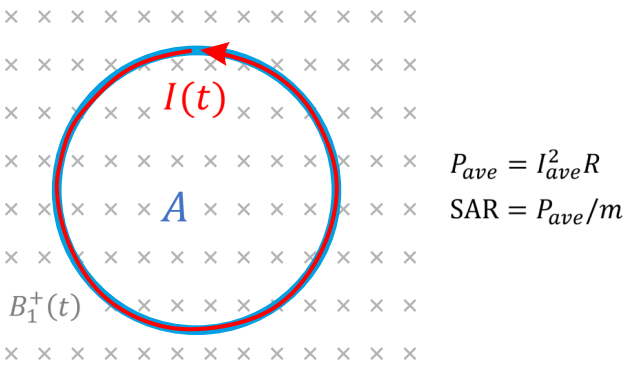


FIG. 1. Simplified 2D model of SAR, neglecting the capacitive effects and displacement currents. The conductive loop in the sample is marked in blue, with an area of A and a resistance R. The induced current is marked in red. This 2D model is inspired by Ref. [35].

amplitude during the rf pulse are negligible compared with its carrier frequency $|dB_1^+(t)|/dt \ll |\omega \cdot B_1^+(t)|$.

Although the calculation of SAR in the human body is more complex, Eq. (14) is sufficient to illustrate and investigate the relevant factors that determine how SAR limitations affect the maximum obtainable SNR_t. When applying MR measurement on humans, it is important to note that it is not possible to change the value of σ, A, and m. Hence, to reduce SAR, one can only reduce ω or B_1^+, or increase TR, so that

$$SAR \propto \frac{\omega^2 \int_0^{T_p} B_1^+(t)^2 dt}{\mathrm{TR}}. \tag{15}$$

For a given nominal flip angle and pulse shape, the rf-pulse bandwidth is proportional to the above integral term

$$\Delta\omega_{rf} \propto \int_0^{T_p} B_1^+(t)^2 dt. \tag{16}$$

H. Scaled rf pulse with magnetic field strength

Since the Larmor frequencies ω for all spin systems increase proportionally to B_0, the pulse bandwidth $\Delta\omega_{rf}$ must be scaled by the same B_0-scaling factor to maintain consistent chemical shift displacement artifacts. Additionally, for adiabatic pulses, it is assumed that their adiabaticity [36–38] should remain unchanged across different magnetic field strengths. Pulses that satisfy both criteria are referred to as *scaled rf pulses*, for which

$$\Delta\omega_{rf} \propto B_0. \tag{17}$$

Therefore,

$$SAR \propto \frac{\omega^2 \int_0^{T_p} B_1^+(t)^2 dt}{\mathrm{TR}} \propto \frac{\omega^2 \Delta\omega_{rf}}{\mathrm{TR}} \propto \frac{B_0^3}{\mathrm{TR}}. \tag{18}$$

III. RESULTS

In order to systematically analyze the relationship between SNR_t and B_0, this paper analyzes three different experimental boundary conditions: (**I**) fixed TA, constant T_1, and constant B_0, (**II**) maximum SAR, fixed TA, B_0-scaled rf-pulse bandwidth $\Delta\omega_{rf}$, and constant T_1 but varying B_0, and (**III**) maximum SAR, fixed TA, B_0-scaled rf-pulse bandwidth $\Delta\omega_{rf}$, and B_0 dependent T_1 but varying B_0.

A. Condition I: fixed TA, constant T_1, and constant B_0

In this scenario, the total acquisition time is fixed while both the longitudinal relaxation time (T_1) and the magnetic field strength (B_0) remain constant. Under these conditions, the normal saturation effect is observed: repeated excitations lead to incomplete recovery of the equilibrium magnetization, resulting in a progressive reduction in signal intensity. Consequently, the SNR_t decreases as the repetition time (TR) increases.

Figure 2 illustrates the signal intensity within one TR (left-hand side panel) and the corresponding SNR_t as a function of TR (right-hand side panel) under these fixed conditions.

When TR exceeds five times the T_1, the system is considered fully relaxed and the saturation effects are minimal. In this case, the F-factor approaches unity, i.e.,

$$F \simeq 1, (\mathrm{TR} > 5T_1). \tag{19}$$

Under these conditions, Eq. (13) simplifies to the following:

$$\mathrm{SNR}_t|_{TA} \propto \frac{B_0}{\sqrt{\mathrm{TR}}}. \tag{20}$$

This relationship reflects the typical saturation behavior in MRS: as TR increases, the number of averages within a fixed acquisition time decreases, leading to a reduction in SNR_t. These equations, with the trends shown in Fig. 2, demonstrate that longer TRs lead to diminished SNR_t due to fewer repetitions, despite full magnetization recovery.

B. Condition II: maximum SAR, fixed TA, B_0-scaled rf-pulse bandwidth $\Delta\omega_{rf}$, and constant T_1 but varying B_0

Here, we investigate the effect of increasing B_0 on the SNR_t where we additionally assume that the pulse sequence is applied at maximum tolerable SAR but with a scaled rf-pulse bandwidth $\Delta\omega_{rf}$ proportional to B_0 to maintain identical spectral coverage Δppm. Furthermore, here we assume that the T_1 does not change as a function of B_0, while keeping the total acquisition time TA constant at all examined B_0. Finally, all the excitations are carried out at the respective Ernst flip angles.

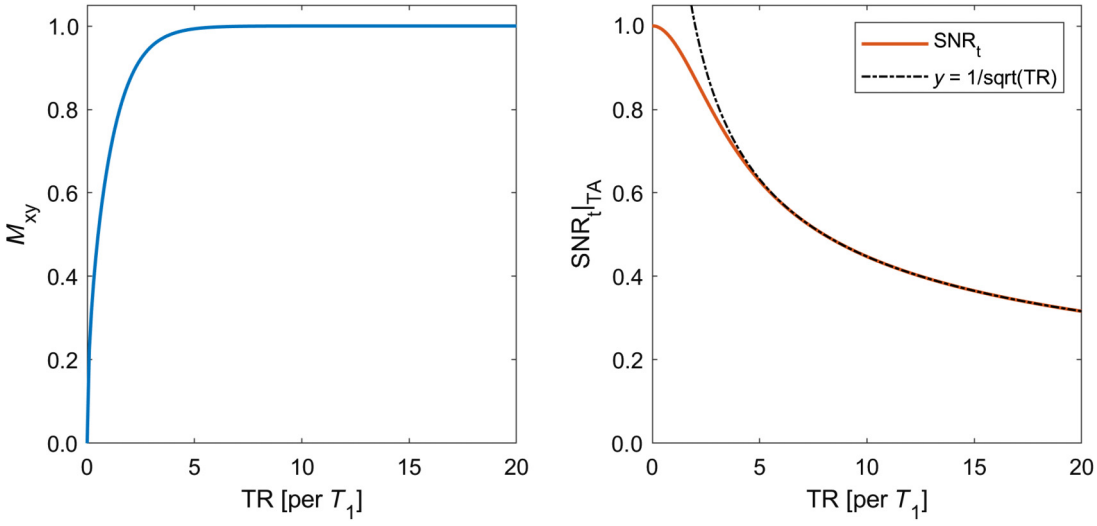


FIG. 2. Simulations of the expected transverse magnetization and SNR$_t$ under the assumptions of (i) a fixed total acquisition time TA, (ii) a constant T_1, and (iii) a constant B_0. (left) Signal of an SVS sequence within one TR with an Ernst angle excitation. (right) Variable SNR$_t$ as a function of TR: the total acquisition time is fixed, so that the shorter the TR, the more repetitions of the excitation (the number of repetitions = TA/TR).

As concluded from the analysis of condition I above, $\mathrm{SNR}_t|_{TA}$ always decreases with increasing TR. Therefore, the optimal SNR$_t$ with fixed TA ($\mathrm{SNR}_t|_{TA,opt}$) for any given SVS sequence is achieved at the shortest possible TR. However, in practice, this minimum TR is constrained by the maximum tolerable SAR. Under these conditions, the optimal $\mathrm{SNR}_t|_{TA,opt}$ can again be expressed as follows [the same as with Eq. (13)]:

$$\mathrm{SNR}_t|_{TA,opt} \propto \frac{B_0 F(B_0)}{\sqrt{\mathrm{TR}}}, \tag{21}$$

and, according to Eq. (18), the maximum tolerable $SAR_{\max}$ is proportional to

$$SAR_{\max} \propto \frac{B_0^3}{\mathrm{TR}}. \tag{22}$$

In Eq. (22), the maximum tolerable SAR (i.e., $SAR_{\max}$), as defined by standard IEC 60601-2-33 [34], is considered constant under the assumption of a fixed organ and a healthy subject. By substitution of Eq. (22) into Eq. (21), the following expression for the optimal SNR$_t$ with fixed TA and the maximum tolerable SAR ($\mathrm{SNR}_t|_{TA,opt,\max Sar}$) is obtained:

$$\mathrm{SNR}_t|_{TA,opt,maxSar} \propto \frac{B_0 \cdot F(B_0)}{\sqrt{B_0^3/SAR_{\max}}} \propto \frac{F(B_0)}{\sqrt{B_0}}. \tag{23}$$

Again note that, in this expression, F is a function of B_0. For a given SVS sequence with maximum SAR at a magnetic field strength B_0, with substitution of the F-factor given by Eq. (9), we find the following expression for $\mathrm{SNR}_t|_{TA,opt,\max Sar}$:

$$\begin{aligned}\mathrm{SNR}_t|_{TA,opt,maxSar} &= S_0 \cdot \frac{F(B_0)}{\sqrt{B_0}} = S_0 \cdot \frac{1}{\sqrt{B_0}} \\ &\cdot \frac{1-\mathrm{e}^{-\mathrm{TR}/T_1}}{1-\cos(\arccos(e^{-\mathrm{TR}/T_1}))\cdot e^{-\mathrm{TR}/T_1}} \sin(\arccos(e^{-\mathrm{TR}/T_1}))\end{aligned} \tag{24}$$

Here, S_0 is the initial voltage measured by the receiver system, which is a constant that does not depend on the sequence parameters and magnetic field. If the magnetic field B_0 is increased by a factor f, we find

$$B_0(f) = f\ B_{0,0}, \tag{25}$$

where $B_{0,0}$ represents the reference magnetic field strength, defined as the lowest B_0 value in the analysis ($f = 1$). In addition, we refer to the shortest TR at maximum SAR for a pulse sequence at $B_{0,0}$ as reference TR (denoted as TR_0). According to Eq. (22),

$$\mathrm{TR}_e = \mathrm{TR}_0 \left(\frac{B_0}{B_{0,0}}\right)^3 = \mathrm{TR}_0 f^3, \tag{26}$$

where TR_e is the effective TR, which is the shortest TR at maximum SAR for a pulse sequence at B_0. By substitution

of Eqs. (25) and (26) into Eq. (24), we discover

$$\mathrm{SNR}_t|_{TA,opt,maxSar} = S_0 \frac{1}{\sqrt{f\,B_{0,0}}} \frac{1-\mathrm{e}^{-f^3\mathrm{TR}_0/T_1}}{1-\cos(\arccos(e^{-f^3\mathrm{TR}_0/T_1}))e^{-f^3\mathrm{TR}_0/T_1}} \times \sin(\arccos(e^{-f^3\mathrm{TR}_0/T_1})). \quad (27)$$

Figure 3 shows the $\mathrm{SNR}_t|_{TA,opt,maxSar}$ changes as a function of f with different reference values TR_0. The variable $\mathrm{SNR}_t|_{TA,opt,maxSar}$ is normalized to one at $f = 1$. Given that the maximum SAR is constant for all B_0, the shorter the TR_0, the lower the absorbed rf energy per TR is. The lower the absorbed rf energy per TR of the sequence, the greater the SNR_t, as can be seen in Fig. 3 when the magnetic field strength B_0 is increased. From this figure, it is evident that in the case of long TR_0 ($\mathrm{TR}_0 \geq 3T_1$), there is no further gain in SNR_t to be expected in the case when the magnetic field strength is increased. The reason for this is that, in this regime, the $\mathrm{SNR}_t|_{TA,opt,\max Sar}$ decreases with the square root of f [Eq. (28)], i.e.,

$$\mathrm{SNR}_t|_{TA,opt,\max Sar}(f) \simeq S_0 \frac{1}{\sqrt{f\,B_{0,0}}}, \quad (28)$$

The $\mathrm{SNR}_t|_{TA,opt,\max Sar}$ is reached at f_{opt}, which corresponds to the following:

$$B_{0,opt} = f_{opt} B_{0,0}, \quad (29)$$

$$\mathrm{TR}_{e,opt} = f_{opt}^3 \mathrm{TR}_0. \quad (30)$$

where $\mathrm{TR}_{e,opt}$ is the optimal effective TR (in short: optimal TR) at optimal magnetic field strength $B_{0,opt}$.

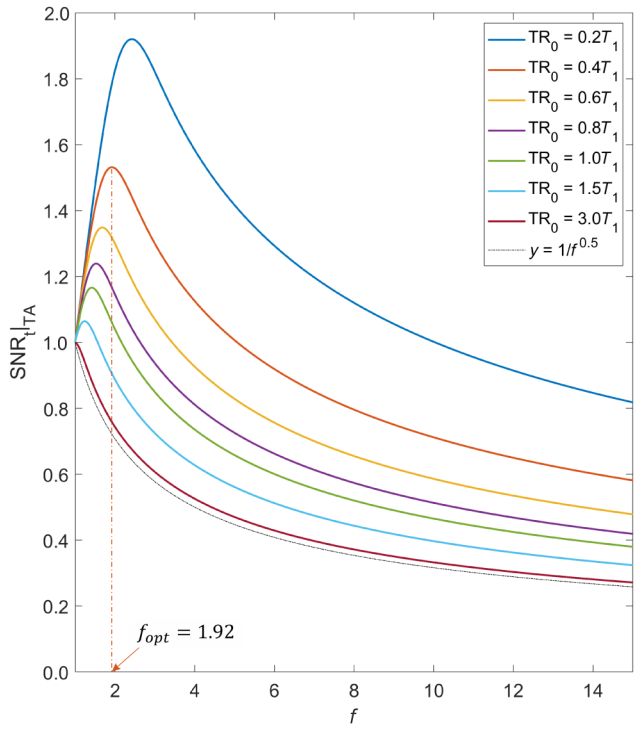


FIG. 3. Optimal SNR per unit time as a function of magnetic field B_0 with constant T_1. The optimal SNR per unit time for different reference TR_0 is normalized at $B_{0,0}$. The total acquisition time TA is assumed to be constant for all the computations, with the spectra acquired at maximum tolerable SAR. For instance, in the case of $\mathrm{TR}_0 = 0.4T_1$, the optimal $f_{opt} \simeq 1.92$, which corresponds to an optimal effective $\mathrm{TR}_{e,opt} = f_{opt}^3 \mathrm{TR}_0 = f_{opt}^3 0.4T_1 \simeq 2.85T_1$.

C. Condition III: maximum SAR, fixed TA, B_0-scaled rf-pulse bandwidth $\Delta\omega_{rf}$, B_0 dependent T_1 but varying B_0

We will now investigate the dependency of SNR_t dependence on T_1, i.e., $T_1 = T_1(B_0)$. As far as we know, for proton spectroscopy, there are some experimentally measured T_1 at different field strengths where T_1 grows with increasing B_0 [32,39,40], but no established analytical equation for the relationship between longitudinal relaxation time T_1 *in vivo* and magnetic field B_0 [40]. By contrast, certain nuclei, such as 31P, exhibit decreasing T_1 at higher B_0 due to the chemical shift anisotropy effect [41]. To proceed, we adopt a parameterized model for the B_0 dependence of T_1 [40], i.e.,

$$T_1(f) = T_{1,0} f^{\alpha}. \quad (31)$$

Again, f is the increase factor by which the magnetic field B_0 is multiplied, $T_{1,0}$ is the reference relaxation time, and α is a constant parameter. It is noteworthy that some experimental studies suggest that α is around 1/3 for a proton but varies from metabolite to metabolite.

In order to illustrate the effect of B_0-dependent T_1 on the $\mathrm{SNR}_t|_{TA,opt,\max Sar}$, we performed two series of simulations. In the first series, we assume that $T_1 \propto \sqrt{B_0}$ and, in the second series, we assume that $T_1 \propto B_0$. For each assumption, we attempted to determine the value of $\mathrm{TR}_{e,opt}$ that maximizes $\mathrm{SNR}_t|_{TA,opt,\max Sar}$. Figure 4 shows $\mathrm{SNR}_t|_{TA,opt,\max Sar}$ with α equal to 0.5 and 1, respectively. As α increases, T_1 also increases with rising B_0, resulting in a reduced $\mathrm{SNR}_t|_{TA,opt,\max Sar}$. The underlying reasons for this behavior will be elaborated in the subsequent discussion.

We further investigated the effect of increasing α with a reference $\mathrm{TR}_0 = 0.5T_{1,0}$, in order to evaluate the general effect of $T_1(\alpha)$ on the $\mathrm{SNR}_t|_{TA,opt,\max Sar}$. Figure 5 shows the $\mathrm{SNR}_t|_{TA,opt,\max Sar}$ simulation results, which were performed with a reference $\mathrm{TR}_0 = 0.5T_{1,0}$, and variable $\alpha \in [0.1, 0.7]$ is the protonlike case, where T_1 increases with B_0, and $\alpha \in [-2.1, -0.3]$ for the 31P-like case, where T_1 decreases with B_0. A larger α not

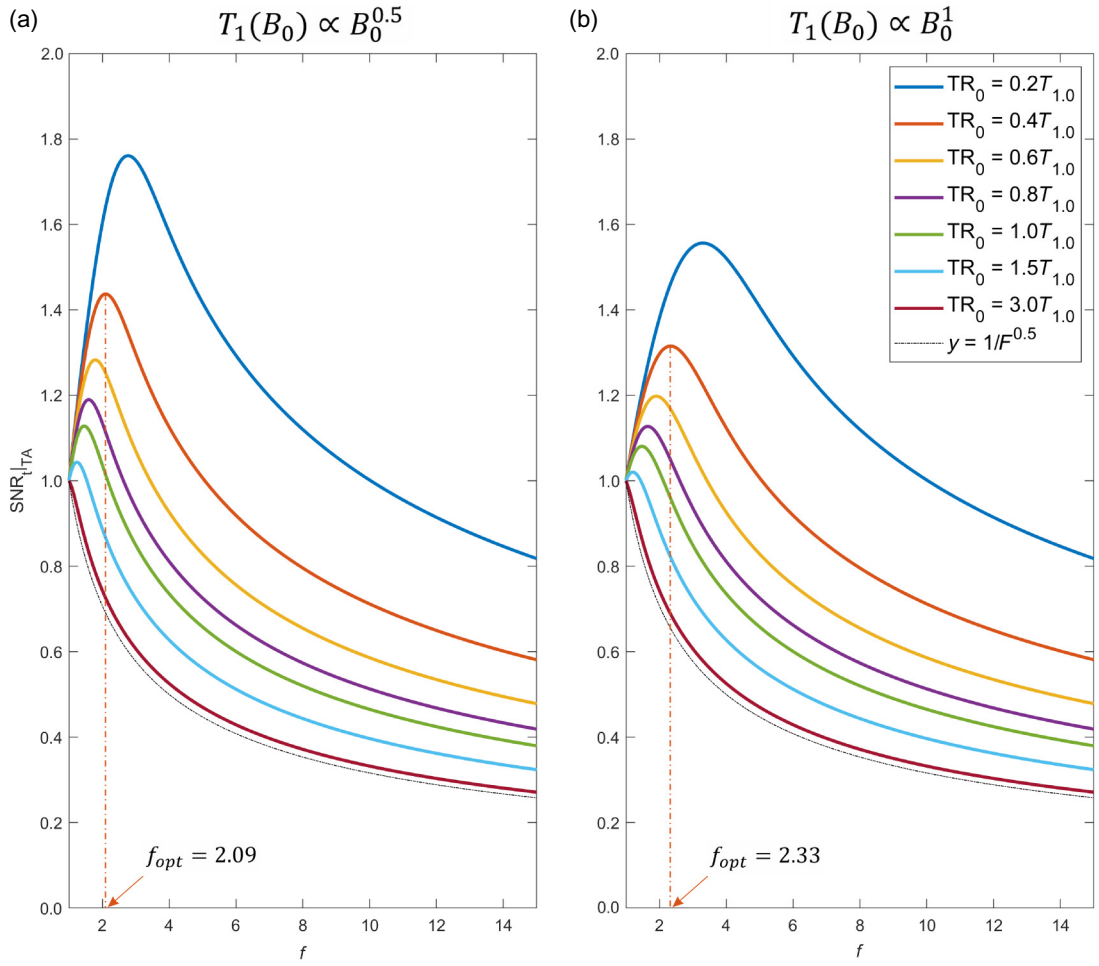


FIG. 4. Variable $\mathrm{SNR}_t|_{TA,opt,\max Sar}$ as a function of magnetic field B_0 with increasing T_1, assuming constant total acquisition time, TA, and acquisition at maximum tolerable SAR: (a) T_1 is proportional to $B_0^{0.5}$ and (b) T_1 is proportional to B_0. For example, (I) in the case of $T_1(B_0) \propto B_0^{0.5}$ and $\mathrm{TR}_0 = 0.4T_{1,0}$ (orange line), f_{opt} is 2.09, which corresponds to the optimal effective $\mathrm{TR}_{e,opt} = f_{opt}^3\,\mathrm{TR}_0 = f_{opt}^3\,0.4T_{1,0} \simeq 3.67T_{1,0} \simeq 2.54T_1$ and (II) in the case of $T_1(B_0) \propto B_0^1$ and $\mathrm{TR}_0 = 0.4T_{1,0}$ (orange line), f_{opt} is 2.33, which corresponds to the optimal effective $\mathrm{TR}_{e,opt} = f_{opt}^3\,\mathrm{TR}_0 = f_{opt}^3\,0.4T_{1,0} \simeq 5.07T_{1,0} \simeq 2.17T_1$.

only reduces $\mathrm{SNR}_t|_{TA,opt,\max Sar}$ but also increases the optimal field strength, $B_{0,opt} \propto f_{opt}$, at which this maximum is reached.

To illustrate the influence of α on $\mathrm{SNR}_t|_{TA,opt,\max Sar}$, we selected $\alpha = 0.3$ and 0.5 as numerical examples, along with the corresponding optimal scaling factor f_{opt} and optimal effective repetition time TR ($\mathrm{TR}_{e,opt}$), as summarized in Tables I and II. For instance, consider an SVS sequence with the following parameters at a reference magnetic field strength of $B_{0,0} = 1.5$ T: $T_{1,0} = 1$ s and $\mathrm{TR}_0 = 0.2T_{1,0} = 0.2$ s. In the scenario where $\alpha = 0.3$, the pulse bandwidth-scaled version of this sequence achieves its $\mathrm{SNR}_t|_{TA,opt,\max Sar}$ at $f_{opt} = 2.61$, corresponding to a field strength of $B_0 = f_{opt}B_{0,0} = 3.915$ T. The optimal effective TR is $\mathrm{TR}_{e,opt} = 3.56$ s, which is 17.8 times longer than TR_0. At this optimal field strength, the $\mathrm{SNR}_t|_{TA,opt,\max Sar}$ is increased by a factor of 1.83 compared with its value at 1.5 T.

IV. DISCUSSION

We first discuss the $\mathrm{SNR}_t|_{TA,opt,\max Sar}$ results of condition II, i.e., the spectroscopy pulse sequence is applied at fixed maximum SAR, fixed TA, constant T_1, B_0-scaled rf-pulse bandwidth $\Delta\omega_{RF}$, and varying B_0. Under these conditions, $\mathrm{SNR}_t|_{TA,opt,\max Sar}$ shows a single maximum as a function of B_0, as shown in Fig. 3. This means that, for a sequence with a short reference TR_0 (and TR_0 is the shortest possible TR, limited by SAR limitation, at current reference magnetic field $B_{0,0}$), there exists a maximum SNR per time unit $\mathrm{SNR}_t|_{TA,\max}$ as a function of the magnetic field B_0. This is because the factor $F(B_0)$ increases

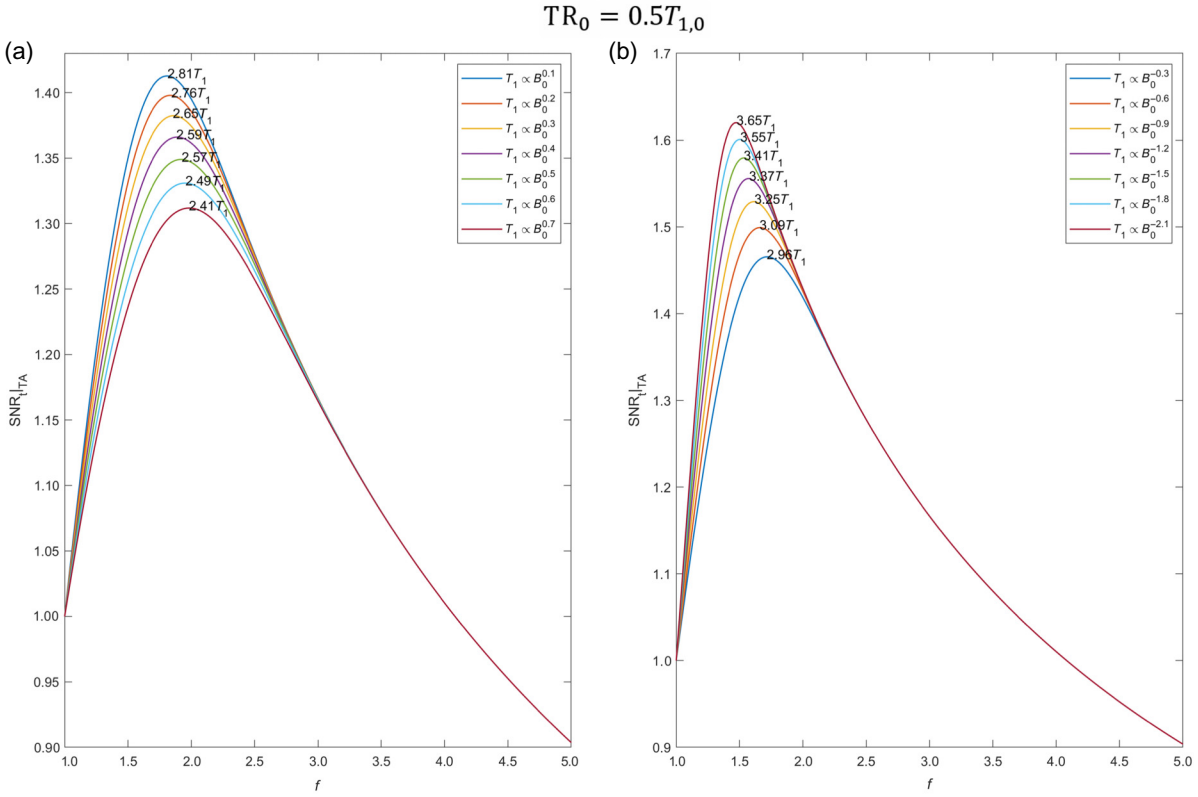


FIG. 5. Variable $\mathrm{SNR}_t|_{TA,opt,\max Sar}$ as a function of variable α-values. The total acquisition time, TA, is the assumed constant, with spectra acquired at maximum tolerable SAR. (a) Optimal effective $\mathrm{TR}_{e,opt}$ at the optimal magnetic field are 2.81, 2.76, 2.65, 2.59, 2.57, 2.49, and $2.41T_1$ for $\alpha = 0.1$, 0.2, 0.3, 0.4, 0.5, 0.6, and 0.7, respectively. (b) Optimal effective $\mathrm{TR}_{e,opt}$ at optimal magnetic field are 2.96, 3.09, 3.25, 3.37, 3.41, 3.55, and $3.65T_1$ for $\alpha = -0.3$, -0.6, -0.9, -1.2, -1.5, -1.8, and -2.1, respectively.

TABLE I. Values of $\mathrm{SNR}_t|_{TA,opt,\max Sar}$ and the corresponding optimal f and optimal effective TR for two different α values. The values are valid under the assumption of constant total acquisition time, TA, acquired at the maximum tolerable SAR.

	$\alpha = 0.3$			$\alpha = 0.5$		
$\mathrm{TR}_0[T_{1,0}]$	f_{opt}	$\mathrm{TR}_{e,opt}$ [TR_0]	$\mathrm{SNR}_t|_{TA,opt,\max Sar}$	f_{opt}	$\mathrm{TR}_{e,opt}$ [TR_0]	$\mathrm{SNR}_t|_{TA,opt,\max Sar}$
0.2	2.61	17.8	1.83	2.77	21.3	1.76
0.4	2.02	8.22	1.48	2.10	9.24	1.44
0.6	1.74	5.25	1.31	1.79	5.69	1.28
0.8	1.56	3.80	1.21	1.59	4.04	1.19
1.0	1.44	2.99	1.14	1.46	3.09	1.13
1.5	1.24	1.91	1.05	1.24	1.91	1.04
2.0	1.11	1.38	1.01	1.10	1.35	1.01
	$\alpha = -0.9$			$\alpha = -2.1$		
$\mathrm{TR}_0[T_{1,0}]$	f_{opt}	$\mathrm{TR}_{e,opt}$ [TR_0]	$\mathrm{SNR}_t|_{TA,opt,\max Sar}$	f_{opt}	$\mathrm{TR}_{e,opt}$ [TR_0]	$\mathrm{SNR}_t|_{TA,opt,\max Sar}$
0.2	2.04	8.52	2.13	1.76	5.47	2.32
0.4	1.71	4.96	1.66	1.54	3.63	1.77
0.6	1.54	3.63	1.44	1.42	2.89	1.51
0.8	1.43	2.94	1.30	1.34	2.43	1.36
1.0	1.35	2.48	1.22	1.29	2.14	1.26
1.5	1.22	1.80	1.09	1.18	1.66	1.12
2.0	1.13	1.44	1.04	1.12	1.41	1.05

TABLE II. Illustrative example translating the values from Table I into practical units, based on an SVS sequence at a reference field strength $B_{0,0} = 1.5T$ and $T_{1,0} = 1$ s.

	$\alpha = 0.3$			$\alpha = 0.5$		
$TR_0[s]$	$B_{0,opt}[T]$	$TR_{e,opt}$ $[s]$	$SNR_t\|_{TA,opt,\max Sar}$	$B_{0,opt}[T]$	$TR_{e,opt}$ $[s]$	$SNR_t\|_{TA,opt,\max Sar}$
0.2	3.92	3.56	1.83	4.16	4.26	1.76
0.4	3.03	3.29	1.48	3.15	3.69	1.44
0.6	2.61	3.15	1.31	2.68	3.42	1.28
0.8	2.34	3.04	1.21	2.39	3.24	1.19
1.0	2.16	2.99	1.14	2.19	3.09	1.13
1.5	1.86	2.86	1.05	1.86	2.86	1.04
2.0	1.67	2.75	1.01	1.66	2.69	1.01
	$\alpha = -0.9$			$\alpha = -2.1$		
$TR_0[s]$	$B_{0,opt}[T]$	$TR_{e,opt}$ $[s]$	$SNR_t\|_{TA,opt,\max Sar}$	$B_{0,opt}[T]$	$TR_{e,opt}$ $[s]$	$SNR_t\|_{TA,opt,\max Sar}$
0.2	3.06	1.70	2.13	2.64	1.09	2.32
0.4	2.56	1.98	1.66	2.31	1.45	1.77
0.6	2.31	2.18	1.44	2.14	1.74	1.51
0.8	2.15	2.35	1.30	2.02	1.95	1.36
1.0	2.03	2.48	1.22	1.93	2.14	1.26
1.5	1.82	2.70	1.09	1.78	2.49	1.12
2.0	1.69	2.87	1.04	1.68	2.81	1.05

faster than $\sqrt{B_0}$ up to the optimal magnetic field $B_{0,opt}$ [Eq. (23)], i.e.,

$$\frac{d\mathrm{SNR}_t|_{TA,opt,maxSar}}{dB_0} = \frac{d\left(F(B_0)/\sqrt{B_0}\right)}{dB_0} = \begin{cases} > 0, & B_0 < B_{0,opt} \\ = 0, & B_0 = B_{0,opt} \\ < 0, & B_0 > B_{0,opt} \end{cases}. \tag{32}$$

For $B_0 < B_{0,opt}$, the increase of $\mathrm{SNR}_t|_{TA,opt,\max Sar}$ is primarily driven by the SNR gain due to the rising B_0. When $B_0 > B_{0,opt}$ the saturation of the spin system begins to counteract and eventually dominates the B_0-related SNR increase, leading to a net decrease in SNR per unit of measurement time.

The optimal effective TR ($TR_e = f^3 TR_0$) for a sequence at the optimal magnetic field $B_{0,opt}$ with a constant T_1 typically falls around the range of $2.8T_1 - 3T_1$ (see Fig. 3). Thus, for sequences with the shortest possible TR, but still greater than $3T_1$, increasing the magnetic field B_0 further yields no additional gain in SNR per unit time.

To recall, for condition III, we additionally assume that T_1 of the metabolites are B_0 dependent as well, i.e., $T_1 = T_1(B_0)$. As shown in Fig. 4, in the case of $TR_0 = 0.4T_{1,0}$, the optimal $TR_{e,opt}$ values are $3.67T_{1,0}$ and $5.07T_{1,0}$ (note, $T_{1,0}$ is constant) for $T_1 \propto B_0^{0.5}$, B_0^1, respectively. This means, as α increases, so does the optimal TR ($TR_{e,opt}$).

We further compare the optimal $TR_{e,opt}$ with the varying $T_1(\alpha)$ at optimal magnetic field $B_{0,opt}$ in Fig. 5. In general, the increase of the α results in the growth of $B_{0,opt}$ and, thus, the increase of $TR_{e,opt}$, and the increase of $T_1(B_{0,opt})$. More specifically, $T_1(\alpha, B_{0,opt})$ grows with α but faster than the optimal TR [Eq. (33)]. Consequently, the ratio of $TR_{e,opt}$ to T_1 decreases with increasing α (Fig. 5).

The values of $TR_{e,opt}$ in Fig. 5 are compared with the field-dependent $T_1(\alpha)$ instead of constant $T_{1,0}$ at the corresponding optimal field $B_{0,opt}$. Generally, a larger α leads to a higher $B_{0,opt}$, which in turn raises both $TR_{e,opt}$ and $T_1(B_{0,opt})$. However, because $T_1(B_{0,opt})$ grows more rapidly than $TR_{e,opt}$ [see Eq. (33)], the ratio $TR_{e,opt}(\alpha, B_{0,opt})/T_1(\alpha, B_{0,opt})$ decreases as α increases. This trend is clearly illustrated in Fig. 5 and can be expressed as

$$\frac{d(TR_{e,opt}(\alpha, B_{0,opt})/T_1(\alpha, B_{0,opt}))}{d\alpha} < 0. \tag{33}$$

In clinical practice of proton spectroscopy, many SVS sequences have a TR of approximately 3 s or more at 3 T [42], which is longer than $2T_1$ at this field strength. Therefore, further gains in SNR per unit time (SNR_t) are not expected when scaling such sequences to higher magnetic field strengths, as indicated in Table I. Specifically, for a sequence with $TR = 2T_1$ at maximum SAR, the additional gain in SNR_t from increasing B_0 is only 1%, assuming $T_1 \propto B_0^\alpha$ with $\alpha = [0.3, 0.5]$, and 4–5% for $\alpha = [-0.9, -2.1]$. The reason for this is that the bandwidth of the rf pulses also scales with B_0 causing the effective TR to increase with B_0^3.

To illustrate the simulated results of the theoretical model, we consider a practical example (Table II) using an SVS sequence at a reference magnetic field ($B_{0,0} = 1.5$ T) with the following parameters: acquisition time (TA) of

5 min, reference relaxation time ($T_{1,0}$) of 1 s, reference repetition time (TR_0) of 0.4 s, and 750 excitations (repetitions).

A. Case $T_1 \propto B_0^{0.3}$

The variable $SNR_t|_{TA,opt,\max Sar}$ is achieved at an optimal magnetic field of $B_{0,opt}=3.03$ T, with an optimal effective TR ($TR_{e,opt}$) of 3.29 s, and ∼91 excitations (repetitions). At this optimal field strength (3.03 T), $SNR_t|_{TA,opt,\max Sar}$ increases by a factor of approximately 1.48 compared with the reference field ($B_{0,0}$) of 1.5 T.

B. Case $T_1 \propto B_0^{0.5}$

The variable $SNR_t|_{TA,opt,\max Sar}$ occurs at $B_{0,opt}=3.15$ T, with an optimal effective TR of $TR_{e,opt}=3.7$ s and ∼81 excitations (repetitions). In this scenario, $SNR_t|_{TA,opt,\max Sar}$ increases by a factor of approximately 1.44 at the optimal field strength (3.15 T) compared with the reference field (1.5 T).

C. 31P-like case $T_1 \propto B_0^{-0.9}$

The variable $SNR_t|_{TA,opt,\max Sar}$ occurs at $B_{0,opt}=2.56$ T, with an optimal effective TR of $TR_{e,opt}=1.98$ s and ∼152 excitations (repetitions). In this scenario, $SNR_t|_{TA,opt,\max Sar}$ increases by a factor of approximately 1.66 at the optimal field strength (2.56 T) compared with the reference field (1.5 T).

However, as mentioned above, B_1^+ - insensitive SVS sequences, especially those which use slice-selective adiabatic rf pulses (like semi-SADLOVE/LASER [8,9]) are associated with high SAR costs and already require a relatively long TR (usually larger than $1.5T_1$) at 3 T. Therefore, the additional rf power of adiabatic rf pulses at higher B_0 must always be compensated when increasing the main magnetic field B_0. This can either be realized by reducing the rf bandwidth or reducing the rf amplitude (but still above the minimal adiabatic B_1^+ - threshold) or both [11]. However, reducing the rf bandwidth increases chemical shift displacement artifacts, while lowering the rf amplitude (a) for adiabatic pulses enhances their sensitivity to B_1^+ inhomogeneity and (b) for nonadiabatic pulses leads to reduced actual flip angles. Therefore, whether $SNR_t|_{TA,opt,\max Sar}$ gains outweigh the performance loss from rf-pulse compensation remains an open question.

V. LIMITATIONS

A. The T_1-weighted effect with short TR

From Fig. 2, we observe that the shorter the repetition time, the higher the $SNR_t|_{TA,opt}$. However, in practical MR spectroscopy, extremely short TRs are rarely used for SVS sequences, even when SAR constraints are not limiting. This is due to two primary reasons. First, metabolites have varying T_1 times. Using a short TR introduces T_1 weighting into the signal, which leads to differential attenuation of metabolite peaks. This variability complicates quantification and, typically, necessitates additional corrections or assumptions to accurately estimate metabolite concentrations. Second, the actual gain in SNR per unit time becomes marginal as TR decreases below T_1. As shown in Fig. 2 (right panel), the normalized SNR_t approaches one as TR approaches zero. Specifically, the relative SNR_t values are 0.99 at $TR=0.5T_1$, 0.96 at $TR=T_1$, 0.92 at $TR=1.5T_1$, 0.87 at $TR=2T_1$, and 0.78 at $TR=3T_1$. This indicates diminishing returns in SNR_t for very short TRs, with minimal gain but increased susceptibility to T_1 weighting effects. Therefore, in practice, a TR in the range of 1 to $2T_1$ is often selected as a compromise, offering reasonable SNR_t performance while minimizing metabolite-specific T_1 weighting effects and simplifying quantification.

In this study, our goal is to theoretically evaluate the upper bound of SNR_t under idealized conditions. While such assumptions may not reflect common clinical protocols, they are essential for establishing the limits of performance and for guiding future optimizations in clinical MRS acquisition strategies.

B. T_2 decay

The T_2 value also depends on the magnetic field strength. Generally, higher magnetic fields result in shorter T_2 values, further reducing the achievable $SNR_t|_{TA,opt,\max Sar}$ when the magnetic field increases. However, the *TE* used in SVS can vary depending on the specific metabolites of interest. For instance, the short *TE* (<35 ms) is typically employed to maximize SNR for major metabolites (such as NAA, Cho, and Cr), whereas a relatively long *TE* (68–144 ms) is required for detecting *J*-coupled metabolites (such as GABA, 2HG, and Lac) in spectral editing techniques. Thus, the effect of T_2 is not included in this work since the analysis presented here is most general and does not target a particular *TE*. Instead, this study provides a theoretical upper bound for $SNR_t|_{TA,opt,\max Sar}$ that is valid across all echo times and can be scaled for specific T_2/TE accordingly.

C. CSI and other types of fast MRSI

One key assumption of this work is that the total acquisition time is fixed and multiple averages are acquired. The other key assumption is the application of the sequence at maximum tolerable SAR. The number of averages for SVS is inversely proportional to the TR, calculated as the number of averages = *TA*/TR. If chemical shift imaging (CSI) [26] or other magnetic resonance spectroscopic imaging [43] protocols involve multiple averages, the analysis presented here would also apply to those cases. However, in most practical scenarios, these sequences are acquired with

only a single average, placing them outside the scope of this analysis presented here. Additionally, in the case of fast MRSI [43], the acquired spectral bandwidth becomes a critical limiting factor at higher magnetic fields. Therefore, extending this analysis to fast MRSI protocols would require the explicit incorporation of the effect of spectral bandwidth.

VI. CONCLUSION

This paper presented a theoretical model for the SNR per unit of the acquisition time as a function of increasing B_0. Under the conditions (1) a fixed TA, (2) maximum SAR constraints, (3) the bandwidth of an rf-pulse scaled with a magnetic field strength, (4) maintenance of adiabaticity when using adiabatic pulses, and (5) PRESS- or (semi)SADLOVE/LASER-type SVS sequences, the SNR per unit time unit shows very little to no improvement, or may even decrease, if the TR at maximum SAR exceeds $2T_1$ as the magnetic field strength increases.

ACKNOWLEDGMENTS

The funding was provided by the Schweizerischer Nationalfonds zur Förderung der Wissenschaftlichen Forschung (Grants No. SNSF-182569 and No. SNSF-207997).

DATA AVAILABILITY

The data that support the findings of this article are openly available [44].

[1] W. A. Edelstein, G. H. Glover, C. J. Hardy, and R. W. Redington, The intrinsic signal-to-noise ratio in NMR imaging, Magn. Reson. Med. **3**, 604 (1986).
[2] J. A. Helpern, The promise of high-field-strength MR imaging., AJNR Am. J. Neuroradiol. **24**, 1738 (2003).
[3] I. Tkáč, G. Öz, G. Adriany, K. Uğurbil, and R. Gruetter, In vivo ^{1}H NMR spectroscopy of the human brain at high magnetic fields: Metabolite quantification at 4T vs. 7T, Magn. Reson. Med. **62**, 868 (2009).
[4] R. Pohmann, O. Speck, and K. Scheffler, Signal-to-noise ratio and MR tissue parameters in human brain imaging at 3, 7, and 9.4 tesla using current receive coil arrays, Magn. Reson. Med. **75**, 801 (2016).
[5] J. T. Vaughan, M. Garwood, C. M. Collins, W. Liu, L. DelaBarre, G. Adriany, P. Andersen, H. Merkle, R. Goebel, M.B. Smith, and K. Uğurbil, 7T vs. 4T: RF power, homogeneity, and signal-to-noise comparison in head images, Magn. Reson. Med. **46**, 24 (2001).
[6] M. E. Ladd, P. Bachert, M. Meyerspeer, E. Moser, A. M. Nagel, D. G. Norris, S. Schmitter, O. Speck, S. Straub, and M. Zaiss, Pros and cons of ultra-high-field MRI/MRS for human application, Prog. Nucl. Magn. Reson. Spectrosc. **109**, 1 (2018).
[7] G. H. Glover, T.-Q. Li, and D. Ress, Image-based method for retrospective correction of physiological motion effects in fMRI: RETROICOR, Magn. Reson. Med. **44**, 162 (2000).
[8] J. Slotboom, A. F. Mehlkopf, and W. M. M. J. Bovée, A single-shot localization pulse sequence suited for coils with inhomogeneous RF fields using adiabatic slice-selective RF pulses, J. Magn. Reson. (1969) **95**, 396 (1991).
[9] M. Garwood and L. DelaBarre, The return of the frequency sweep: Designing adiabatic pulses for contemporary NMR, J. Magn. Reson. **153**, 155 (2001).
[10] P. A. Bottomley, Spatial localization in NMR spectroscopy in vivo, Ann. N. Y. Acad. Sci. **508**, 333 (1987).
[11] G. Weng, P. Radojewski, S. Sheriff, C. Kiefer, P. Schucht, R. Wiest, A. A. Maudsley, and J. Slotboom, SLOW: A novel spectral editing method for whole-brain MRSI at ultra high magnetic field, Magn. Reson. Med. **88**, 53 (2022).
[12] G. Öz, D. K. Deelchand, J. P. Wijnen, V. Mlynárik, L. Xin, R. Mekle, R. Noeske, T. W. J. Scheenen, and I. Tkáč, Advanced single voxel ^{1}H magnetic resonance spectroscopy techniques in humans: Experts' consensus recommendations, NMR Biomed. **34**, e4236 (2021).
[13] J. Near, A. D. Harris, C. Juchem, R. Kreis, M. Marjańska, G. Öz, J. Slotboom, M. Wilson, and C. Gasparovic, Preprocessing, analysis and quantification in single-voxel magnetic resonance spectroscopy: experts' consensus recommendations, NMR Biomed. **34**, e4257 (2021).
[14] M. Wilson, *et al.*, Methodological consensus on clinical proton MRS of the brain: Review and recommendations, Magn. Reson. Med. **82**, 527 (2019).
[15] D. I. Hoult and P. C. Lauterbur, The sensitivity of the zeugmatographic experiment involving human samples, J. Magn. Reson. (1969) **34**, 425 (1979).
[16] P. B. Barker, D. O. Hearshen, and M. D. Boska, Single-voxel proton MRS of the human brain at 1.5T and 3.0T, Magn. Reson. Med. **45**, 765 (2001).
[17] K. Kantarci, G. Reynolds, R. C. Petersen, B. F. Boeve, D. S. Knopman, S. D. Edland, G. E. Smith, R. J. Ivnik, E. G. Tangalos, and C. R. Jack, Proton MR spectroscopy in mild cognitive impairment and Alzheimer disease: Comparison of 1.5 and 3T, AJNR Am. J. Neuroradiol. **24**, 843 (2003).
[18] O. Gonen, S. Gruber, B. S. Y. Li, V. Mlynárik, and E. Moser, Multivoxel 3D proton spectroscopy in the brain at 1.5 versus 3.0T: Signal-to-noise ratio and resolution comparison, AJNR Am. J. Neuroradiol. **22**, 1727 (2001).
[19] J. Kim, K.-H. Chang, D. G. Na, I. C. Song, S. J. Kim, B. J. Kwon, and M. H. Han, Comparison of 1.5 and 3 T 1H MR spectroscopy for human brain tumors, Korean J. Radiol. **7**, 156 (2006).
[20] S. Younis, A. Hougaard, C. E. Christensen, M. B. Vestergaard, E. T. Petersen, V. O. Boer, O. B. Paulson, M. Ashina, A. Marsman, and H. B. W. Larsson, Feasibility of glutamate and GABA detection in pons and thalamus at 3 and 7 T by proton magnetic resonance spectroscopy, Front. Neurosci. **14**, 559314 (2020).
[21] S. Pradhan, S. Bonekamp, J. S. Gillen, L. M. Rowland, S. A. Wijtenburg, R. A. E. Edden, and P. B. Barker, Comparison of single voxel brain MRS AT 3 and 7 T using 32-channel head coils, Magn. Reson. Imaging **33**, 1013 (2015).

[22] M. C. Stephenson, Applications of multi-nuclear magnetic resonance spectroscopy at 7T, World J. Radiol. **3**, 105 (2011).
[23] M. Sarracanie and N. Salameh, Low-field MRI: How low can we go? A fresh view on an old debate, Front. Phys. **8**, 172 (2020).
[24] T. C. Arnold, C. W. Freeman, B. Litt, and J. M. Stein, Low-field MRI: Clinical promise and challenges, J. Magn. Reson. Imaging **57**, 25 (2023).
[25] R. Otazo, B. Mueller, K. Uğurbil, L. Wald, and S. Posse, Signal-to-noise ratio and spectral linewidth improvements between 1.5 and 7 Tesla in proton echo-planar spectroscopic imaging, Magn. Reson. Med. **56**, 1200 (2006).
[26] R. Pohmann, M. Von Kienlin, and A. Haase, Theoretical evaluation and comparison of fast chemical shift imaging methods, J. Magn. Reson. **129**, 145 (1997).
[27] T. M. Fiedler, M. E. Ladd, and A. K. Bitz, SAR simulations & safety, Neuroimage **168**, 33 (2018).
[28] B. Guérin, M. Gebhardt, S. Cauley, E. Adalsteinsson, and L. L. Wald, Local specific absorption rate (SAR), global SAR, transmitter power, and excitation accuracy trade-offs in low flip-angle parallel transmit pulse design, Magn. Reson. Med. **71**, 1446 (2014).
[29] J. B. Johnson, Thermal agitation of electricity in conductors, Phys. Rev. **32**, 97 (1928).
[30] H. Nyquist, Thermal agitation of electric charge in conductors, Phys. Rev. **32**, 110 (1928).
[31] R. Pohmann, N. I. Avdievich, and K. Scheffler, Signal-to-noise ratio versus field strength for small surface coils, NMR Biomed. **37**, e5168 (2024).
[32] R. A. de Graaf, P. B. Brown, S. McIntyre, T. W. Nixon, K. L. Behar, and D. L. Rothman, High magnetic field water and metabolite proton T_1 and T_2 relaxation in rat brain in vivo, Magn. Reson. Med. **56**, 386 (2006).
[33] D. K. Deelchand, I. Iltis, and P.-G. Henry, Improved quantification precision of human brain short echo-time ^{1}H magnetic resonance spectroscopy at high magnetic field: A simulation study, Magn. Reson. Med. **72**, 20 (2014).
[34] *IEC 60601-2-33*, 4.0 (International Electrotechnical Commission, Geneva, 2022).
[35] A. D. Elster, *MRIquestions.Com*, (unpublished).
[36] J. Baum, R. Tycko, and A. Pines, Broadband and adiabatic inversion of a two-level system by phase-modulated pulses, Phys. Rev. A (Coll Park) **32**, 3435 (1985).
[37] S. Conolly, G. Glover, D. Nishimura, and A. Macovski, A reduced power selective adiabatic spin-echo pulse sequence, Magn. Reson. Med. **18**, 28 (1991).
[38] P. Balchandani, J. Pauly, and D. Spielman, Designing adiabatic radio frequency pulses using the Shinnar-Le Roux algorithm., Magn. Reson. Med. **64**, 843 (2010).
[39] Y. Li, D. Xu, E. Ozturk-Isik, J. M. Lupo, A. P. Chen, D. B. Vigneron and S. J. Nelson, T1 and T2 metabolite relaxation times in normal brain at 3T and 7T, J. Mol. Imaging Dyn. **002** (2012).
[40] W. D. Rooney, G. Johnson, X. Li, E. R. Cohen, S. Kim, K. Uğurbil, and C. S. Springer, Magnetic field and tissue dependencies of human brain longitudinal ^1H_2O relaxation in vivo, Magn. Reson. Med. **57**, 308 (2007).
[41] W. Bogner, M. Chmelik, A. I. Schmid, E. Moser, S. Trattnig, and S. Gruber, Assessment of ^{31}P relaxation times in the human calf muscle: A comparison between 3 and 7 T in vivo, Magn. Reson. Med. **62**, 574 (2009).
[42] D. Hong, S. Rohani Rankouhi, J.-W. Thielen, J. J. A. van Asten, and D. G. Norris, A comparison of sLASER and MEGA-sLASER using simultaneous interleaved acquisition for measuring GABA in the human brain at 7T, PLoS One **14**, e0223702 (2019).
[43] W. Bogner, R. Otazo, and A. Henning, Accelerated MR spectroscopic imaging—a review of current and emerging techniques, NMR Biomed. **34**, e4314 (2021).
[44] G. Weng and J. Slotboom, Supporting Dataset for: When more is less: Higher magnetic fields and their limited impact on signal-to-noise ratio per unit of acquisition time in unlocalized and single-voxel magnetic resonance spectroscopy, https://doi.org/10.5281/zenodo.17245778 (2025).